

**Supplemental Information**

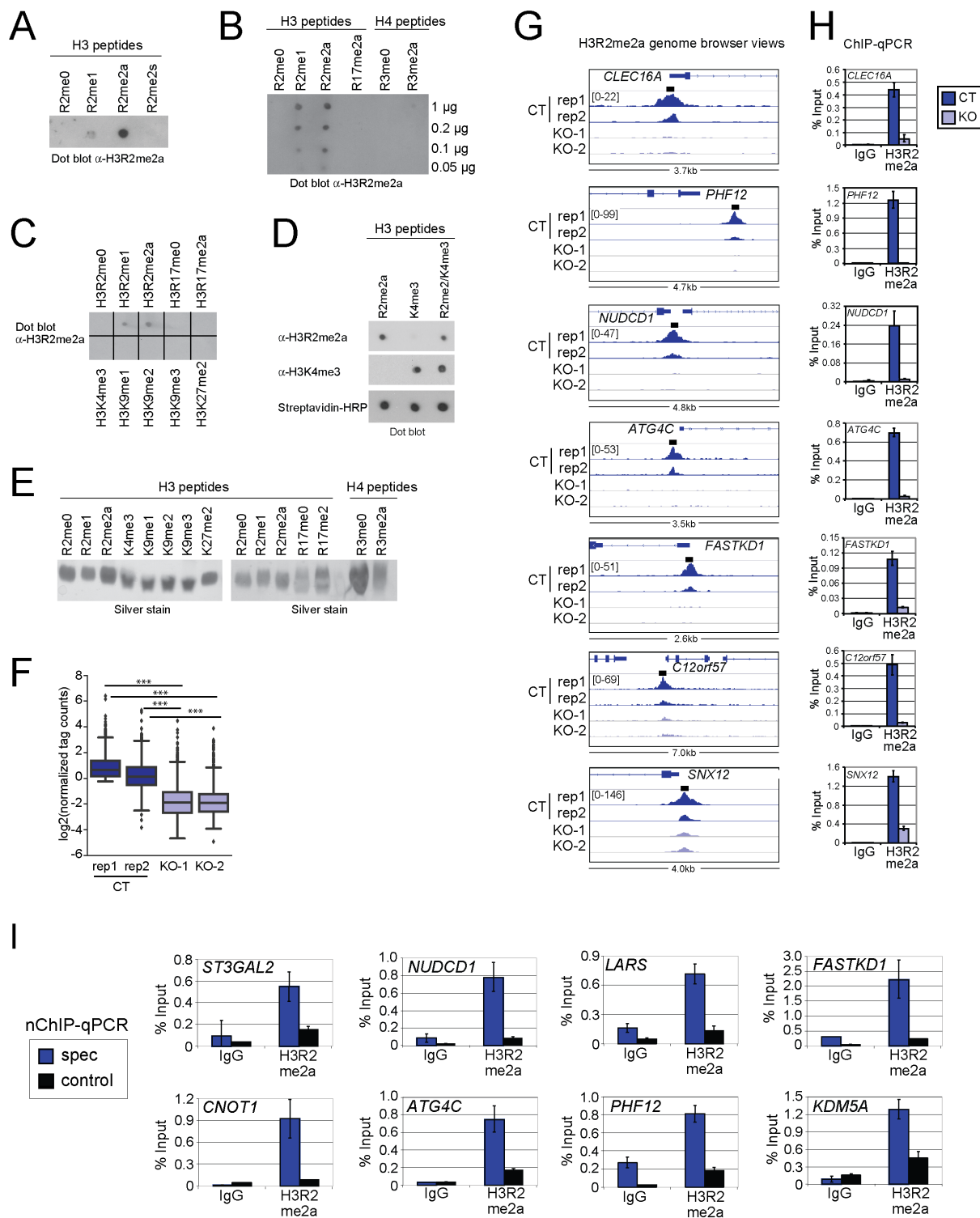
**Genomic Location of PRMT6-Dependent  
H3R2 Methylation Is Linked  
to the Transcriptional Outcome of Associated Genes**

**Caroline Bouchard, Peeyush Sahu, Marion Meixner, René Reiner Nötzold, Marco B. Rust, Elisabeth Kremmer, Regina Feederle, Gene Hart-Smith, Florian Finkernagel, Marek Bartkuhn, Soni Savai Pullamsetti, Andrea Nist, Thorsten Stiewe, Sjaak Philipsen, and Uta-Maria Bauer**

# Supplemental Information

## Supplemental Figures and Legends

### Suppl.Figure S1



### Suppl.Figure S1

**Characterization of the  $\alpha$ -H3R2me2a rat monoclonal antibody by dot blot analyses (A-E) and additional validations of H3R2me2a binding sites in undifferentiated NT2/D1 cells (F-I). Related to Figure 1.**

**A:** H3 peptides (aa 1-8, 1 $\mu$ g each) either unmodified at R2 (R2me0), monomethylated (R2me1), asymmetrically dimethylated (R2me2a) or symmetrically dimethylated (R2me2s) were spotted on nitrocellulose and stained with rat monoclonal  $\alpha$ -H3R2me2a.

**B:** Indicated amounts of H3 peptides (aa 1-30 or 1-24) and H4 peptides (aa 1-15) either unmodified or modified were spotted on nitrocellulose and stained with rat monoclonal  $\alpha$ -H3R2me2a.

**C:** Various H3 peptides (1 $\mu$ g each) either unmodified or modified were spotted on nitrocellulose and stained with rat monoclonal  $\alpha$ -H3R2me2a.

**D:** H3 peptides (aa 1-15 and biotinylated at the C-terminus, 1 $\mu$ g each) modified at R2me2a, K4me3 or double modified (R2me2a/K4me3) were spotted on nitrocellulose and stained with the indicated antibodies or as loading control with streptavidin-HRP (Invitrogen).

**E:** The various H3 and H4 peptides (1 $\mu$ g each, used in A-D) were visualized by SDS-PAGE and silver staining.

**F:** Boxplot analysis illustrates the normalized H3R2me2a tag counts of NT2/D1 CT (two ChIP-seq replicates) and both NT2D1 KO cell lines. \*\*\*:  $p \leq 0.001$  using Welch's t-test.

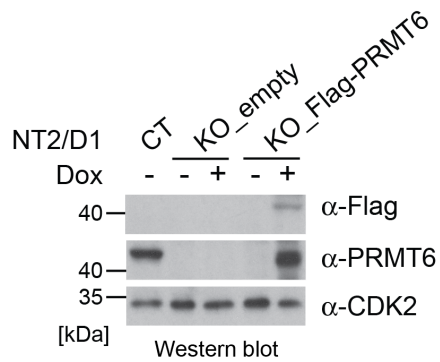
**G:** Genome browser views of the H3R2me2a ChIP-seq data sets of NT2/D1 CT (two replicates) and both KO cell lines depicted for additional gene loci. Positions of amplicons generated by qPCR are depicted as black boxes above the top browser tracks. Data range is indicated in brackets.

**H:** ChIP-qPCR assays were performed in NT2/D1 CT and KO cells (= KO-2, which we employed in all subsequent experiments as PRMT6 knockout cell line) using control antibodies (IgG) and  $\alpha$ -H3R2me2a with primers amplifying the H3R2me2a peaks of the depicted loci (in G). Recruitment is displayed in % input of chromatin (mean  $\pm$  SD of triplicates).

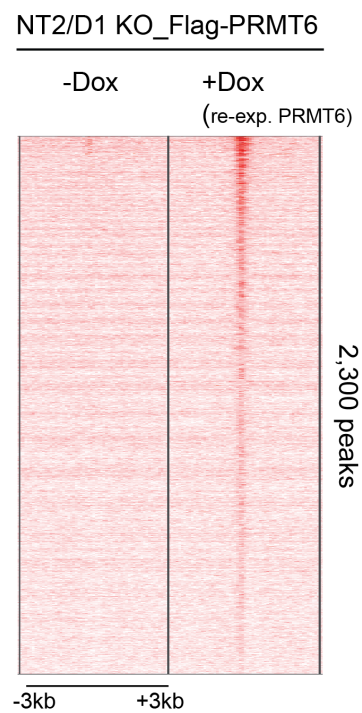
**I:** Native (unfixed) chromatin was isolated from NT2/D1 cells and digested using Micrococcal nuclease (as described in Umlauf et al., 2005). Mononucleosomes were employed in native ChIP (nChIP) experiments using control antibodies (IgG) and  $\alpha$ -H3R2me2a. Subsequently, qPCR assays were performed with primers amplifying either the H3R2me2a peaks (spec) or a nearby control region (control) of the indicated loci. Positions of amplicons generated by qPCR (spec) are depicted in Fig. 1D and S1G. Recruitment is displayed in % input of chromatin (mean  $\pm$  SD of triplicates).

# Suppl. Figure S2

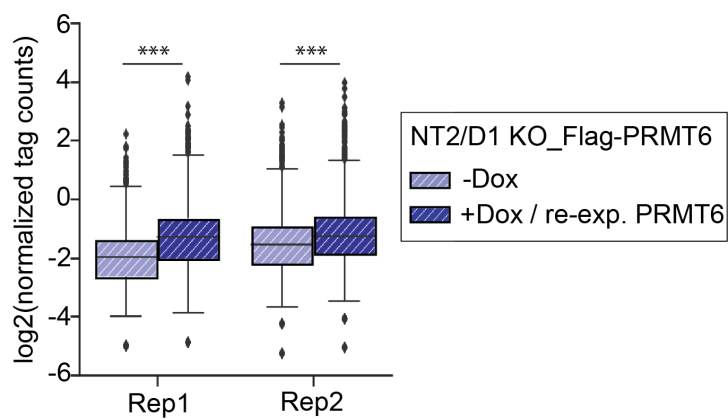
**A**



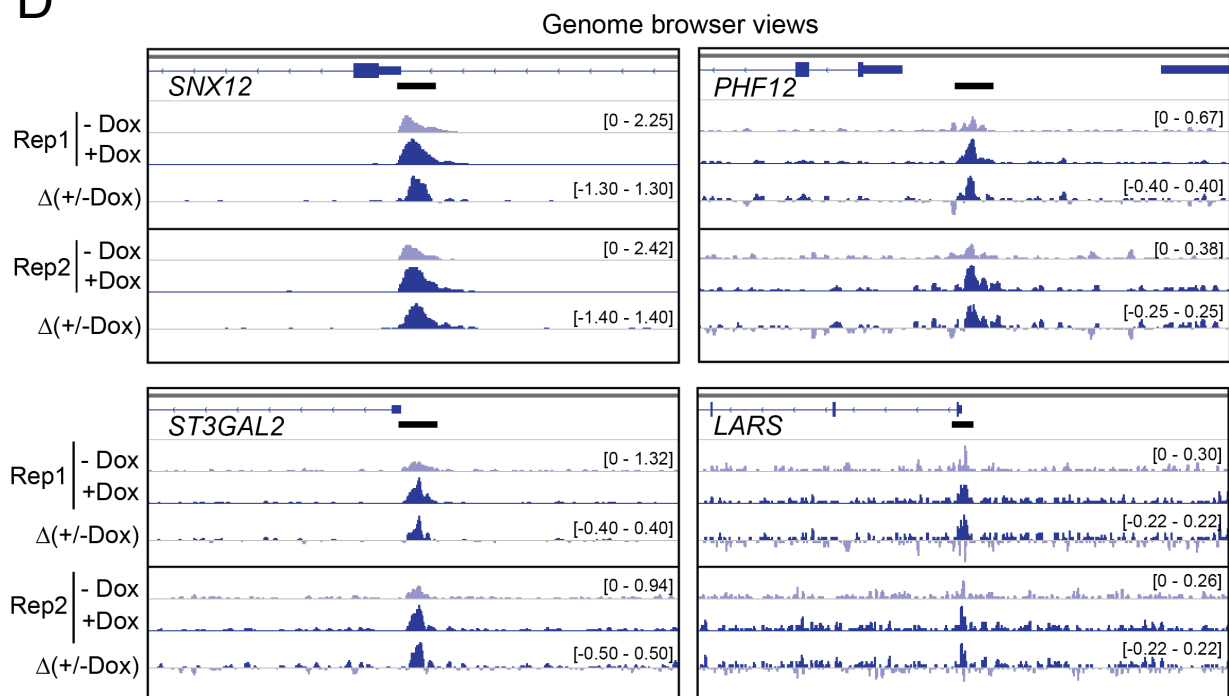
**B**



**C**



**D**





### Suppl.Figure S2

#### Re-expression of PRMT6 in NT2/D1 KO cells and H3R2me2a ChIP-seq analysis. Related to Figure 1.

**A:** Protein extracts of NT2/D1 CT cells and KO cells either infected with pInducer20 empty vector or pInducer20-3xFlag-PRMT6 (-/+ doxycycline for 6 days) were analyzed by Western blot using the indicated antibodies ( $\alpha$ -Flag,  $\alpha$ -PRMT6,  $\alpha$ -CDK2) to monitor doxycycline-inducible expression of Flag-PRMT6 in NT2/D1 KO\_Flag-PRMT6 cells. CDK2 staining served as loading control. Size markers (in kDa) are shown on the left.

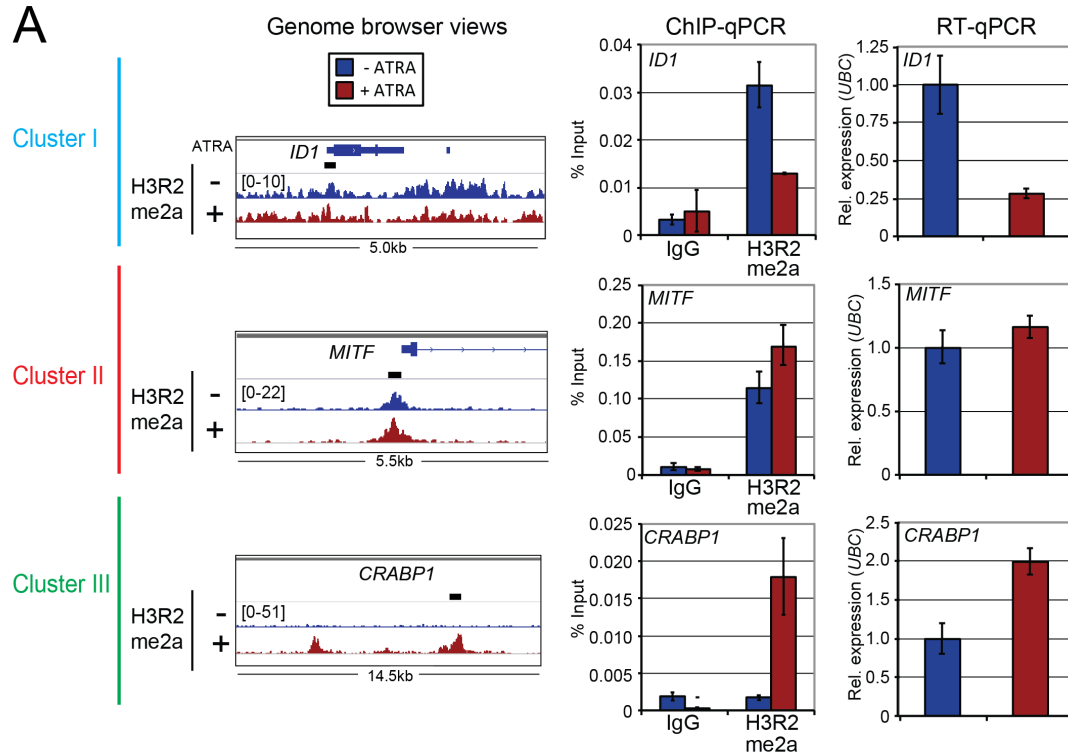
**B:** Heatmap displays the H3R2me2a ChIP-seq signals (replicate 1) in NT2/D1 KO\_Flag-PRMT6 cells +/- doxycycline over the 2,300 binding sites sorted in the descending order of their signal strength (+/- 3kb around the centered summits).

**C:** Boxplot analysis illustrates the normalized H3R2me2a tag counts (of two ChIP-seq replicates) in NT2D1 KO\_Flag-PRMT6 cells in the absence (- doxycycline) or presence (+ doxycycline) of PRMT6 re-expression. \*\*\*:  $p \leq 0.001$  using Welch's t-test.

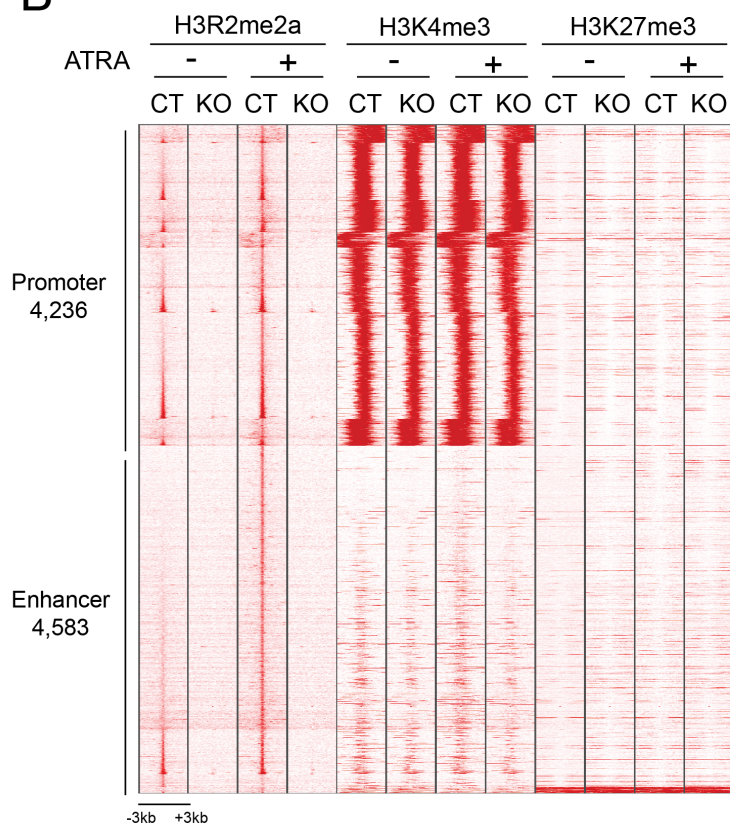
**D:** Genome browser views of the H3R2me2a ChIP-seq data sets in NT2/D1 KO\_Flag-PRMT6 cells (of replicates 1 and 2) +/- doxycycline are depicted for four gene loci. H3R2me2a signal differences between +/- doxycycline ( $\Delta$ +/- Dox) are illustrated in a separate track for each replicate. Positions of H3R2me2a peaks, which show an increased H3R2me2a occupancy upon Flag-PRMT6 expression (+ doxycycline), are highlighted with black boxes above the top browser tracks. Normalized data range is indicated in brackets.

## Suppl.Figure S3

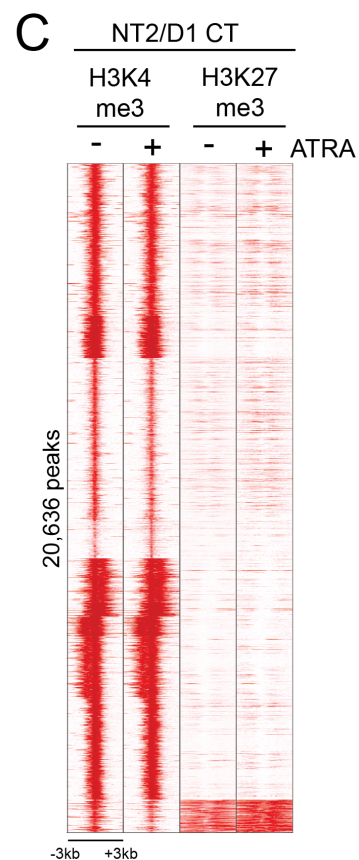
A



B



C



### Suppl.Figure S3

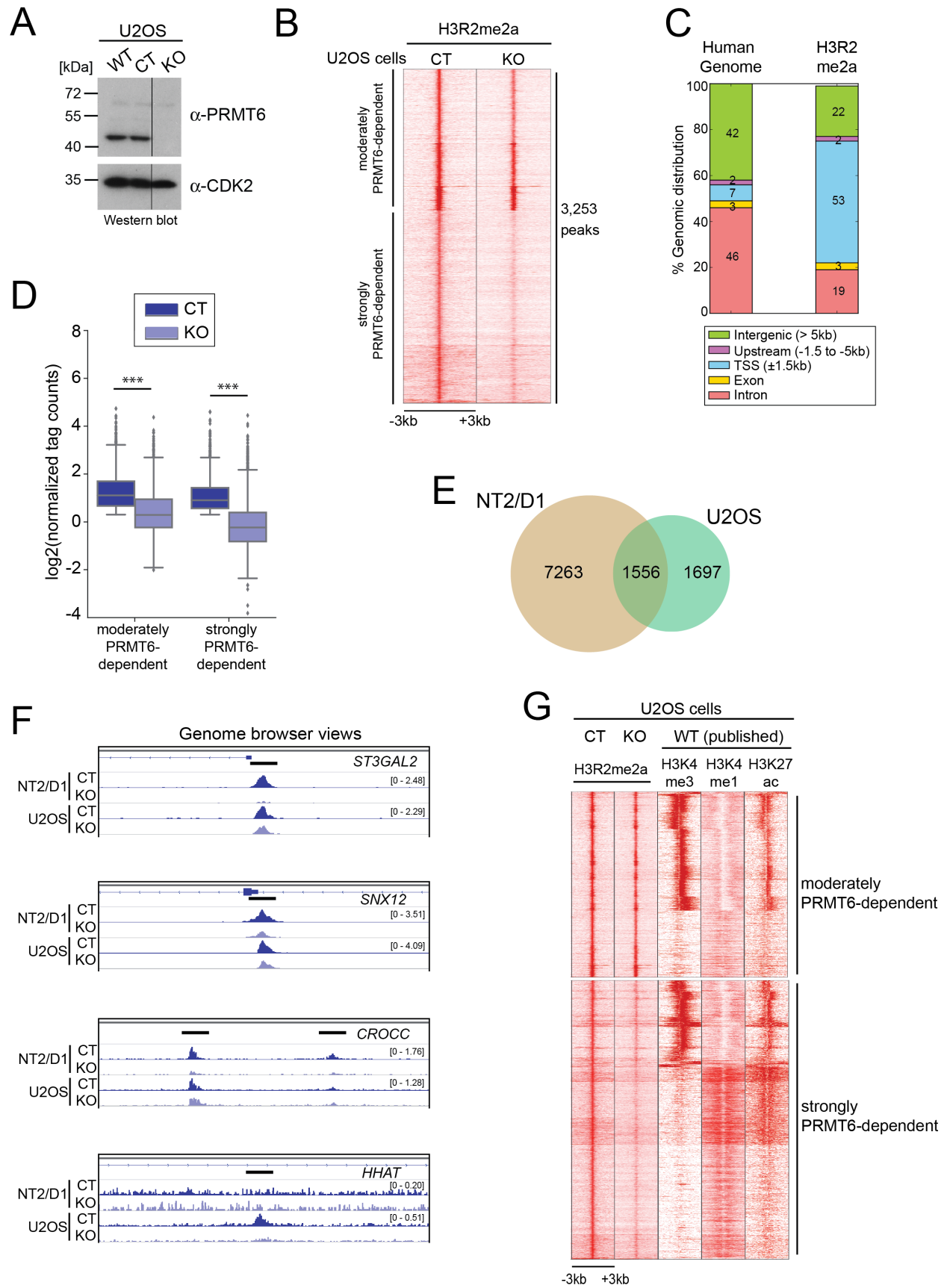
**Additional validations of H3R2me2a binding sites for all three clusters in NT2/D1 CT cells (A) and analysis of a potential bivalency (H3K4me3/H3K27me3 co-occupancy) of H3R2me2a peaks (B, C). Related to Figure 2.**

**A:** Genome browser views of the H3R2me2a ChIP-seq data sets of NT2/D1 CT cells +/- ATRA are depicted for gene loci illustrating the three clusters (left panels): *IDI* (cluster I), *MITF* (cluster II) and *CRABP1* (cluster III) (left panels). Positions of amplicons generated by qPCR are depicted as black boxes above the top browser tracks. Data range is indicated in brackets. ChIP-qPCR assays were performed using control antibodies (IgG) and  $\alpha$ -H3R2me2a and primers amplifying the H3R2me2a peaks of the depicted loci. Recruitment is displayed in % input of chromatin, mean  $\pm$  SD of triplicates (middle panels). Total RNA was analyzed by RT-qPCR for the transcript levels derived from these three gene loci. Values were normalized to *UBIQUITIN* (*UBC*) expression and presented relative to the - ATRA condition, mean  $\pm$  SD of triplicates (right panels).

**B:** Heatmap illustrates the H3R2me2a ChIP signals over 8,819 sites in comparison to the ChIP-seq profile of H3K4me3 and H3K27me3 in NT2/D1 CT and KO cells +/- ATRA with regions classified in promoters (4,236 sites displaying high H3K4me3 occupancy, as shown in Fig. 2D) or enhancers (4,583 sites displaying high H3K4me1/H3K27ac occupancy, as shown in Fig. 2D).

**C:** Heatmap illustrates the H3K4me3 ChIP signals for all 20,636 H3K4me3 peaks in comparison to the H3K27me3 ChIP-seq in NT2/D1 CT cells +/- ATRA, confirming the presence of bivalent loci in NT2/D1 cells, which do not overlap with H3R2me2a sites (as shown in B).

# Suppl.Figure S4



#### **Suppl.Figure S4**

##### **H3R2me2a ChIP-seq analysis in U2OS cells. Related to Figure 2.**

**A:** Protein extracts of U2OS either wild type (WT), *GFP* control gRNA infected (CT) or *PRMT6* gRNAs infected (KO) were analyzed by Western blot using the indicated antibodies ( $\alpha$ -PRMT6,  $\alpha$ -CDK2) to monitor *PRMT6* knockout in the U2OS KO cell clone. CDK2 staining served as loading control. Size markers (in kDa) are shown on the left.

**B:** Heatmap displays the H3R2me2a ChIP-seq signals in U2OS CT and KO cells over the 3,253 binding sites sorted in moderate and strong PRMT6-dependency (+/- 3kb around the centered summits).

**C:** Relative distribution of the 3,253 H3R2me2a peaks in U2OS cells (of B) is shown within different genomic regions compared to the distribution of these regions in the human genome.

**D:** Boxplot analysis illustrates the normalized H3R2me2a tag counts of the ChIP-seq analyses (in B) for moderately and strongly PRMT6-dependent peaks in U2OS CT and KO cells. \*\*\*:  $p \leq 0.001$  using Welch's t-test.

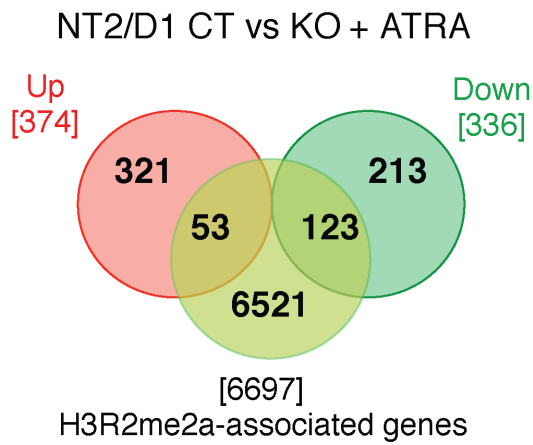
**E:** Venn diagram illustrates the overlap of H3R2me2a binding sites gained from ChIP-seq in NT2/D1 CT and U2OS CT cells.

**F:** Genome browser views of the H3R2me2a ChIP-seq data sets of NT2/D1 CT / KO and U2OS CT / KO cells are depicted for four gene loci. Positions of H3R2me2a peaks, which show a decreased H3R2me2a occupancy upon PRMT6 deletion, are highlighted with black boxes above the top browser tracks. Normalized data range is indicated in brackets. *ST3GAL2*, *SNX12* and *CROCC* represent gene loci with common H3R2me2a peaks in both cell lines. *HHAT* represents a gene locus with a H3R2me2a peak specific for U2OS cells.

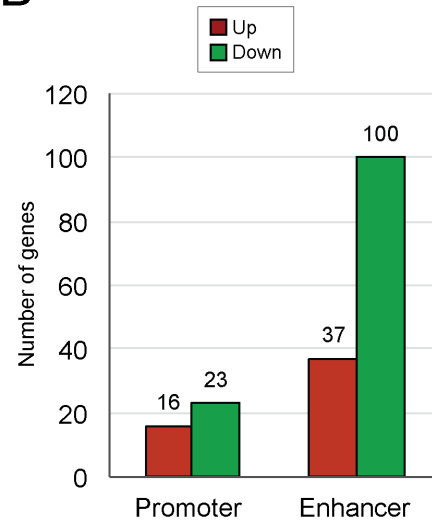
**G:** Heatmap illustrates the H3R2me2a ChIP signals of U2OS CT cells over 3,253 sites in comparison to published ChIP-seq profiles of H3K4me3, H3K4me1 and H3K27ac of U2OS wild type cells (WT) classified in moderately and strongly PRMT6-dependent peaks (as shown in B).

# Suppl.Figure S5

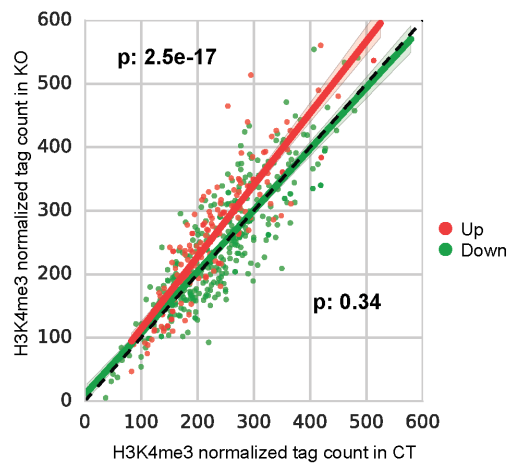
A



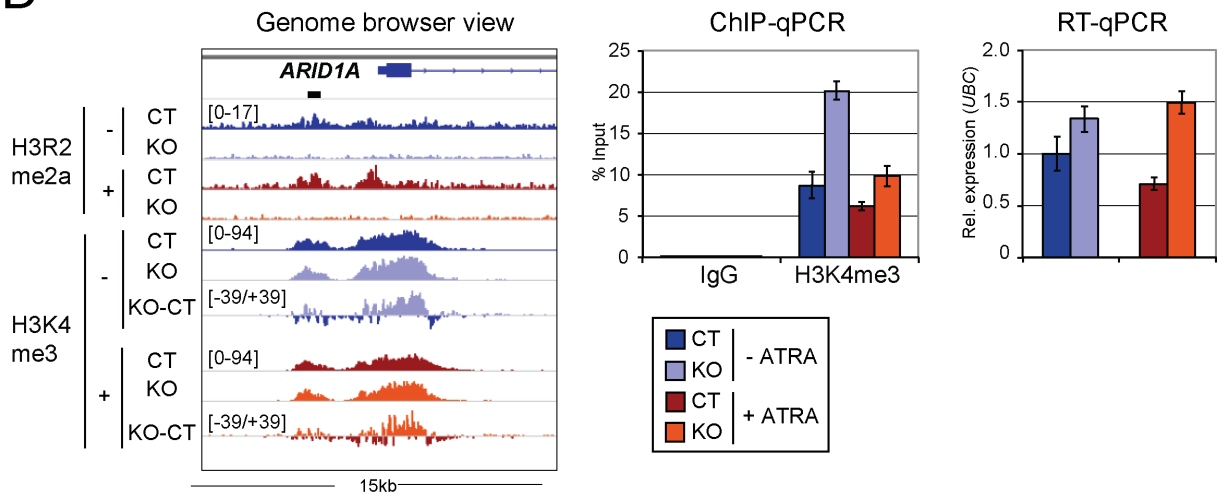
B



C



D



**Suppl.Figure S5**

**RNA-seq analysis of NT2/D1 CT and KO cells + ATRA (A, B) and influence of PRMT6 knockout on H3K4me3 deposition in NT2/D1 cells (C, D). Related to Figures 2 and 3.**

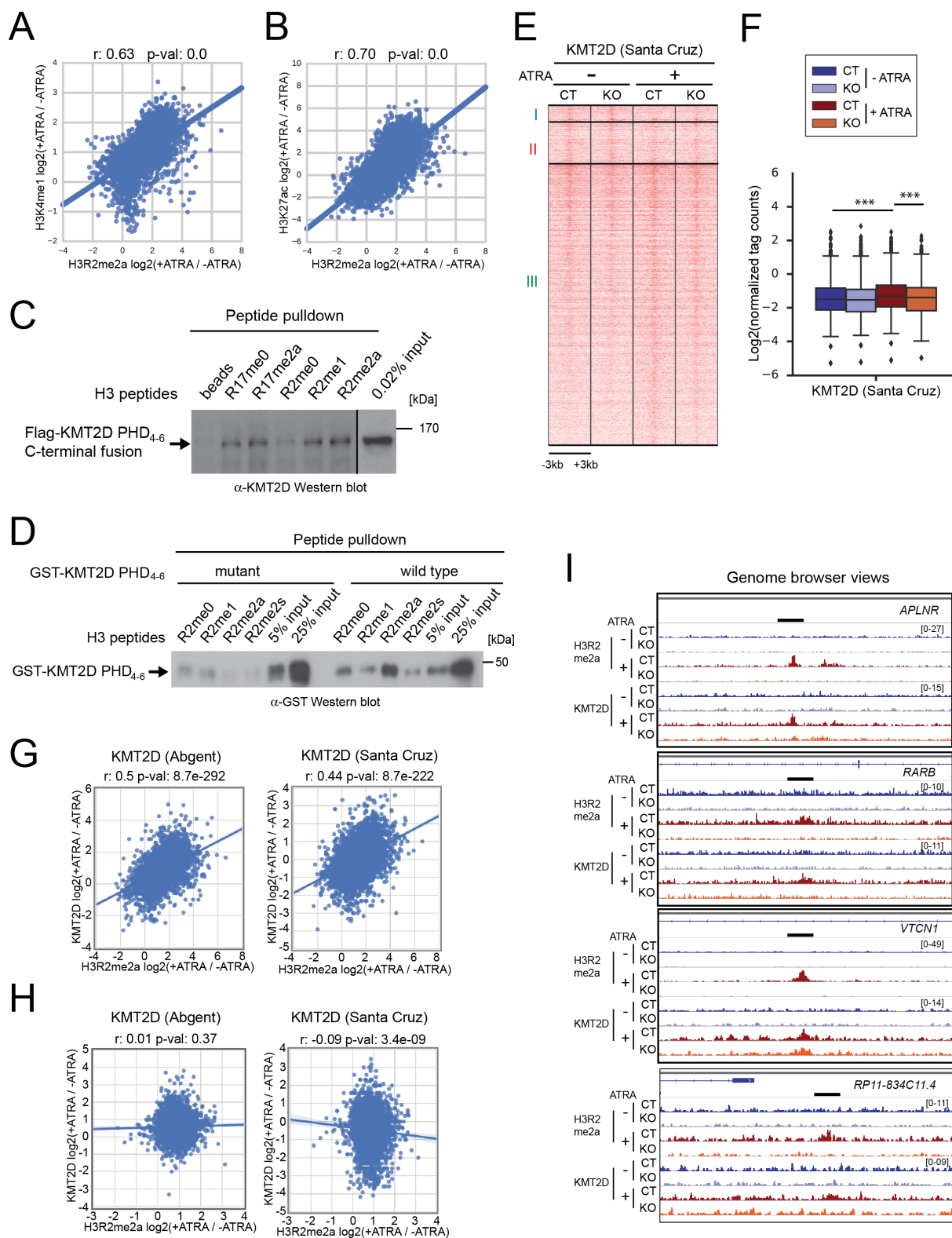
**A:** Venn diagram shows the intersection of differentially expressed genes upon PRMT6 deletion separated in up- and down-regulated genes and genes associated with H3R2me2a binding sites in NT2/D1 CT cells + ATRA.

**B:** Expression changes in NT2/D1 cells + ATRA upon PRMT6 knockout (at least fold change  $\pm 2$  and  $FDR \leq 0.01$ ) are depicted in gene numbers for either promoter-associated or enhancer-associated H3R2me2a binding sites.

**C:** Scatter plot presents the normalized H3K4me3 tag counts for up- (red fitted regression line) and down-regulated (green fitted regression line) genes in NT2/D1 CT versus KO cells. Black dotted diagonal indicates identical levels of the H3K4me3 marks in both cell lines. P-values are depicted (Welch's t-test).

**D:** Genome browser views of the H3R2me2a and H3K4me3 ChIP-seq data sets generated in NT2/D1 CT and KO cells +/- ATRA are shown for the cluster III gene *ARID1A* (left panel). H3K4me3 signal differences between NT2/D1 KO and CT are illustrated in separate tracks (KO-CT). Position of amplicon generated by qPCR is depicted as a black box above the browser track. Data range is indicated in brackets. ChIP-qPCR assays were performed using control antibodies (IgG) and  $\alpha$ -H3K4me3 and primers encompassing the H3R2me2a peak of *ARID1A*. Recruitment is displayed in % input of chromatin, mean  $\pm$  SD of triplicates (middle panel). Total RNA was analyzed by RT-qPCR for transcript levels of *ARID1A*. Values were normalized to *UBIQUITIN* (*UBC*) expression and presented relative to NT2/D1 CT cells -ATRA, mean  $\pm$  SD of triplicates (right panel).

# Suppl.Figure S6





### Suppl.Figure S6

#### Cross-talk between H3R2me2a and the enhancer marks H3K4me1/H3K27ac as well as KMT2D. Related to Figure 4.

**A, B:** Fold change of H3R2me2a levels in NT2/D1 cells  $\pm$  ATRA was plotted versus fold change of H3K4me1 (in A) or H3K27ac (in B) levels for all enhancer peaks. The Spearman correlation coefficient  $r$  and the  $p$ -val are indicated.

**C:** Indicated histone H3 peptides (aa 1-24 for peptides encompassing R17 and aa 1-30 for peptides encompassing R2) were covalently coupled to Sulfolink-beads and incubated with HeLa cell extract overexpressing Flag-KMT2D PHD<sub>4-6</sub> C-terminal fusion protein (Dhar et al., 2012). Pulldown reactions and 0.02% input of cell extract were resolved by SDS-PAGE and analyzed by  $\alpha$ -KMT2D Western blot. Size marker (in kDa) is shown on the right.

**D:** Indicated histone H3 peptides (aa 1-8) were covalently coupled to Sulfolink-beads and incubated with bacterially expressed and purified GST-KMT2D PHD<sub>4-6</sub> mutant (4 mutations/amino acids exchanges in PHD<sub>6</sub>, which have been published to disrupt the KMT2D recognition of the H4 N-terminus (Dhar et al., 2012)) or wild type protein. Pulldown reactions and indicated input of GST-KMT2D proteins were resolved by SDS-PAGE and analyzed by  $\alpha$ -GST Western blot. Size marker (in kDa) is shown on the right.

**E:** Heatmap presents the KMT2D ChIP-seq profile (using the KMTD2 antibody from Santa Cruz) in NT2/D1 CT as well as KO cells  $\pm$  ATRA at the 4,583 enhancer-associated H3R2me2a binding sites (similar to Fig. 4A). These H3R2me2a sites of NT2/D1 CT cells are sorted according to their affiliation to the three clusters.

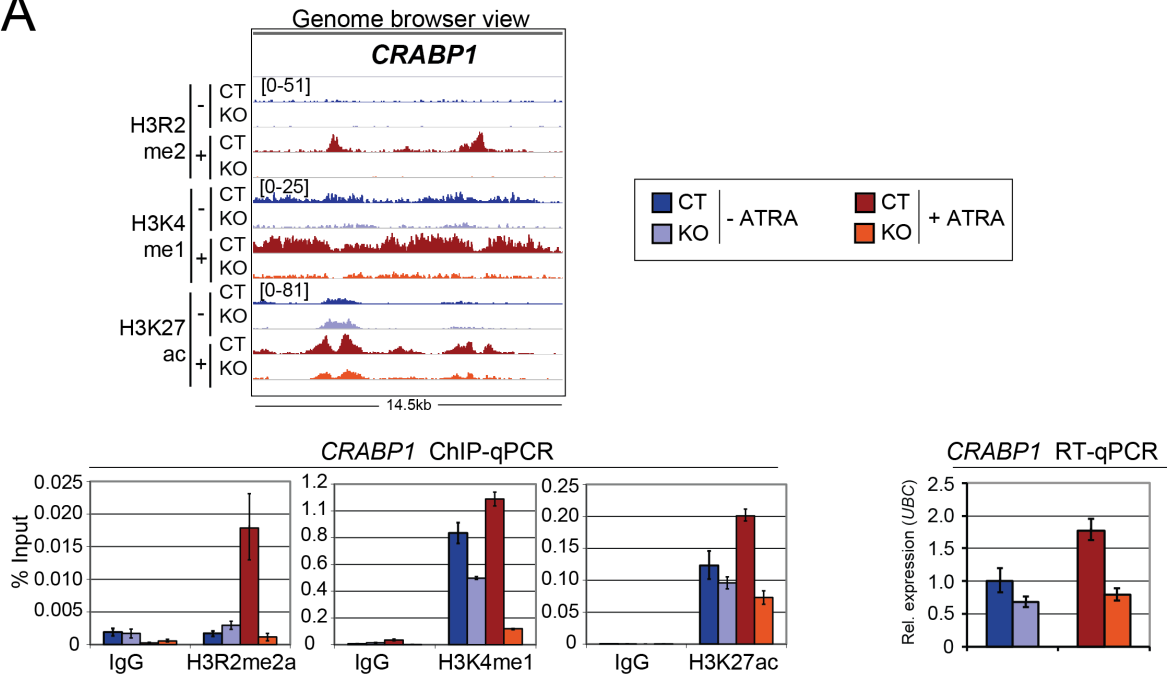
**F:** Boxplot analysis illustrates the normalized tag counts ( $\pm$  2kb centering H3R2me2a peaks) of KMT2D peaks (for samples of E). \*\*\*:  $p \leq 0.001$  using Welch's t-test.

**G, H:** Fold change of H3R2me2a occupancy in NT2/D1 cells  $\pm$  ATRA was plotted versus fold change of KMT2D occupancy (detected using the KMTD2 antibody either from Abgent or from Santa Cruz) for all enhancer peaks (G) and for all promoter peaks (H). The Spearman correlation coefficient  $r$  and the  $p$ -val are indicated. A positive correlation between H3R2me2a and KMT2D occupancy was detectable for H3R2me2a enhancer peaks in G (but not promoter peaks in H).

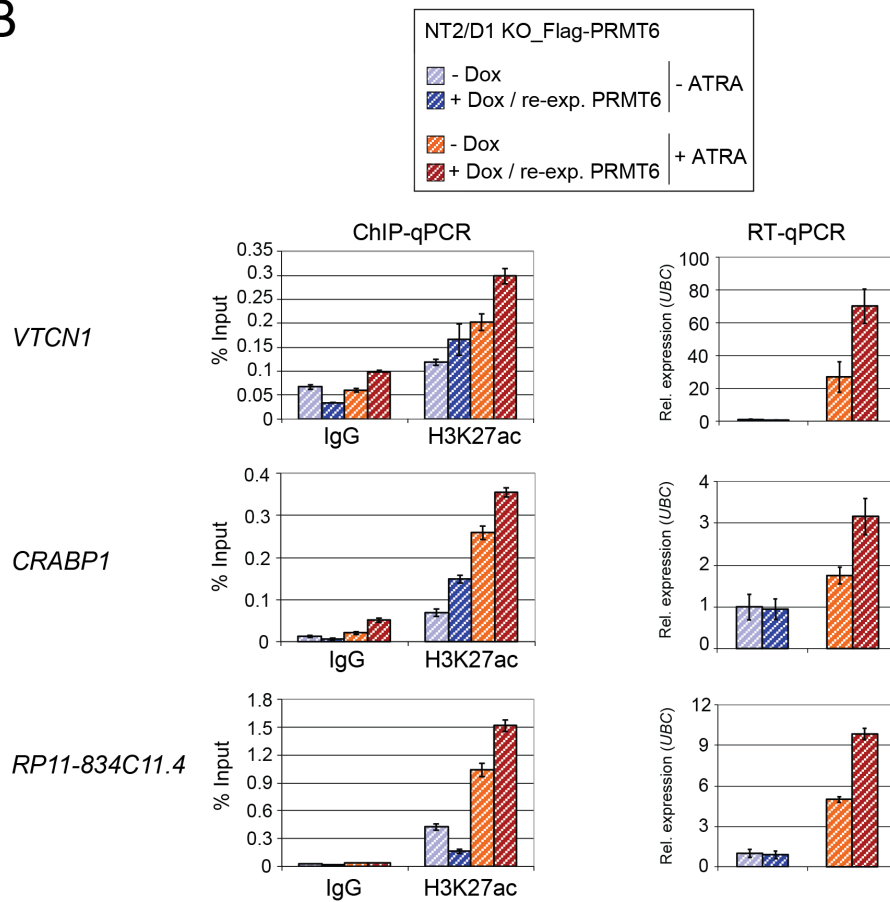
**I:** Genome browser views of H3R2me2a and KMT2D ChIP-seq data sets, which were generated in NT2/D1 CT and KO cells  $\pm$  ATRA, are shown for the indicated gene loci. Positions of co-occurring H3R2me2a and KMT2D peaks, which reveal decreased occupancy upon PRMT6 deletion, are highlighted with black boxes above the top browser tracks. Data range is indicated in brackets.

# Suppl.Figure S7

A



B



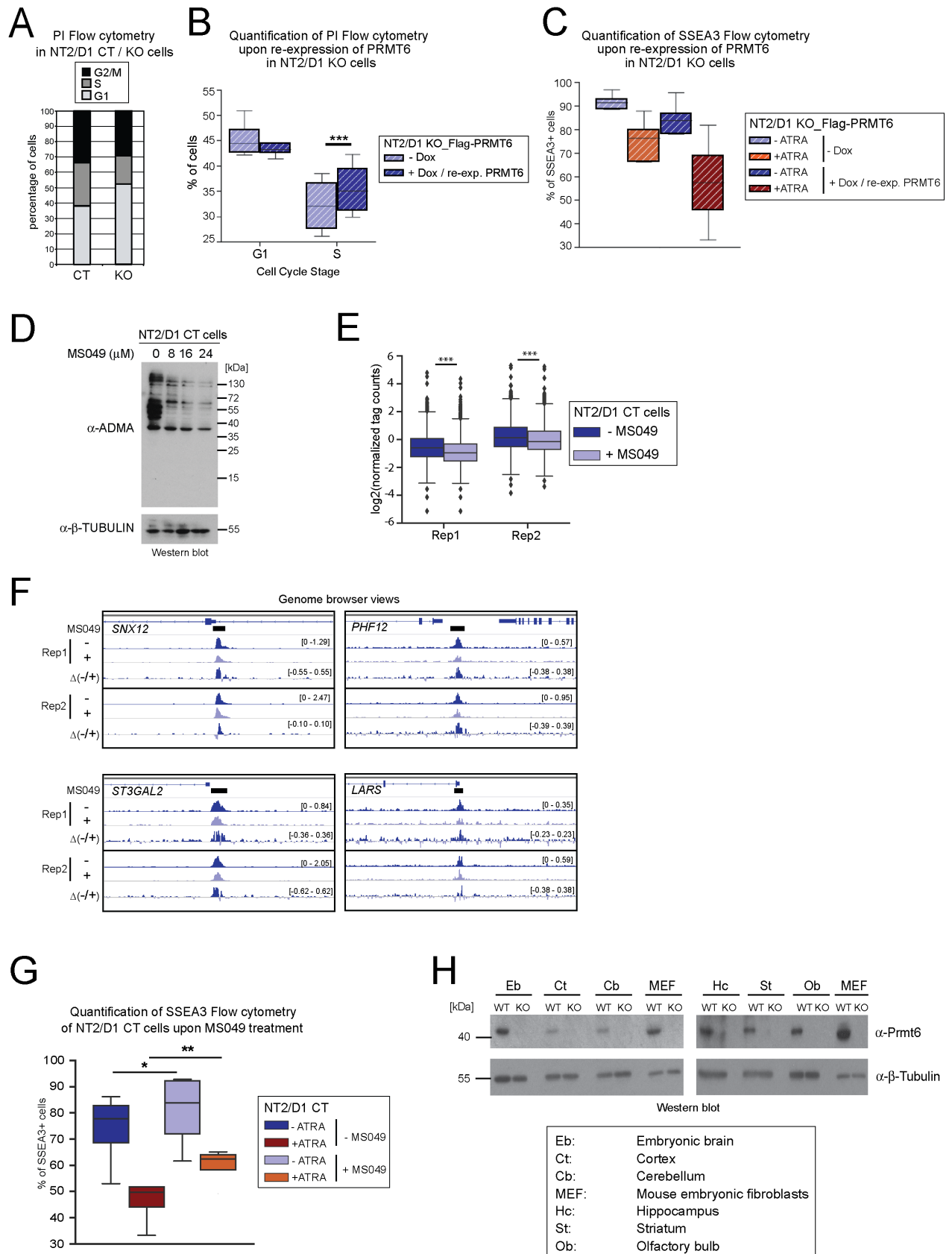
**Suppl.Figure S7**

**Validation of the cluster III gene *CRABP1* by ChIP-qPCR and RT-qPCR (A) and rescue of ATRA-induced H3K27ac deposition and transcriptional activation of target genes in NT2/D1 KO cells upon re-expression of Flag-PRMT6 (B). Related to Figure 5.**

**A:** Genome browser view of the *CRABP1* gene locus is shown for H3R2me2a, H3K4me1 and H3K27ac ChIP-seq data sets generated in NT2/D1 CT and KO cells -/+ ATRA (upper panel). Data range is indicated in brackets. ChIP-qPCR assays were performed in NT2/D1 cells using the indicated antibodies and primers encompassing the histone modification peaks. Recruitment is displayed in % input of chromatin, mean  $\pm$  SD of triplicates (lower left panels). Transcript levels of *CRABP1* was analyzed by RT-qPCR in NT2/D1 CT and KO cells -/+ ATRA. Values were normalized to *UBIQUITIN (UBC)* expression and presented relative to NT2/D1 CT cells - ATRA, mean  $\pm$  SD of triplicates (lower right panel).

**B:** ChIP-qPCR assays were performed in NT2/D1 KO cells in the absence (- doxycycline) or presence (+ doxycycline) of PRMT6 re-expression and in -/+ ATRA conditions using control antibodies (IgG),  $\alpha$ -H3K27ac and primers encompassing the H3K27ac peaks of the three indicated gene loci (corresponding genome browser views are depicted in A and Fig. 5A). Recruitment is displayed in % input of chromatin, mean  $\pm$  SD of triplicates (left panels). Total RNA was analyzed by RT-qPCR for transcript levels of *VTCN1*, *CRABP1* and *RP11-834C11.4*. Values were normalized to *UBIQUITIN (UBC)* expression and presented relative to the -Dox/-ATRA condition, mean  $\pm$  SD of triplicates (right panels).

# Suppl.Figure S8



### Suppl.Figure S8

#### Effect of PRMT6 on the cell cycle distribution and pluripotency/neural differentiation of NT2/D1 cells. Related to Figure 6.

**A:** Cell cycle distribution of NT2/D1 CT and KO cells was analyzed by flow cytometry using propidium iodide (PI) DNA staining.

**B:** NT2/D1 KO\_Flag-PRMT6 cells were cultured in the absence or presence of PRMT6 re-expression (-/+ doxycycline for 6 days). Cell cycle distribution was analyzed by flow cytometry using propidium iodide (PI) DNA staining. The quantification of four independent experiments is displayed. \*\*\*:  $p \leq 0.001$  using paired t-test.

**C:** NT2/D1 KO\_Flag-PRMT6 cells were cultured in the absence or presence of PRMT6 re-expression (-/+ doxycycline for 6 days) and +/- ATRA (last 3 days). The fraction of SSEA3-positive (SSEA3+) cells was measured by flow cytometry. The quantification of four independent experiments is displayed.

**D:** NT2/D1 CT cells were either untreated (0) or treated with the indicated concentrations of MS049 for 3 days. Subsequently, protein extracts were analyzed by Western blot using the indicated antibodies ( $\alpha$ -ADMA,  $\alpha$ -CDK2). CDK2 staining served as loading control. Size markers (in kDa) are shown on the right.

**E:** Boxplot analysis illustrates the normalized H3R2me2a tag counts of two ChIP-seq replicates in NT2/D1 CT cells +/- of 16  $\mu$ M MS049 for 3 days. \*\*\*:  $p \leq 0.001$  using Welch's t-test.

**F:** Genome browser views of the H3R2me2a ChIP-seq data sets of NT2/D1 CT cells +/- 16  $\mu$ M MS049 (replicates 1 and 2 of E) are depicted for four gene loci. H3R2me2a signal differences between +/- MS049 ( $\Delta$ -/+ ) are illustrated in a separate track for each replicate. Positions of H3R2me2a peaks, which show a decreased H3R2me2a occupancy upon MS049 treatment, are highlighted with black boxes above the top browser tracks. Normalized data range is indicated in brackets.

**G:** The fraction of SSEA3-positive (SSEA3+) NT2/D1 CT cells either untreated or treated for 3 days with ATRA, MS049 (16  $\mu$ M) or both was measured by flow cytometry. The quantification of four independent experiments is displayed. \*:  $p \leq 0.05$ ; \*\*:  $p \leq 0.01$  using paired t-test.

**H:** Brain tissue was dissected from *Prmt6* WT and KO mice (either E12.5 cortices pooled from several embryos or the indicated brain areas of adult animals, 16-20 weeks of age), immediately frozen in liquid nitrogen and stored at -80°C. Brain extracts were prepared by homogenizing frozen tissue in ice-cold lysis buffer (50mM Tris/HCl pH 7.4, 150mM NaCl, 0.5% NP-40, 0.1% SDS, plus protease-inhibitors). Furthermore, total protein lysates of MEF cell lines *Prmt6* WT and KO were employed. Protein extracts (20 $\mu$ g per sample) were analyzed by Western blot using  $\alpha$ -PRMT6.  $\beta$ -Tubulin staining served as loading control. Size markers (in kDa) are shown on the left.

## Supplemental Experimental Procedures

### Antibodies

The following antibodies were used: rabbit anti-GST-PRMT6 was produced using His-tagged proteins corresponding to amino acids 60–375 of human PRMT6, rabbit anti-PRMT6 (A300-929A, Bethyl Laboratories), mouse anti- $\beta$ -TUBULIN (MAB3408, Merck Millipore), anti-human CDK2 (sc-163, Santa Cruz Biotechnology), rabbit anti-asymmetrically dimethylated arginine (ADMA, 13522, Cell Signaling), rabbit anti-H3K4me3 (07-473, Merck Millipore), rabbit anti-H3K4me1 (39297, Active Motif), rabbit anti-H3K27ac (39133, Active Motif), rabbit anti-H3K27me3 (07-449, Millipore), rabbit anti-KMT2D (AP6183a, Abgent), rabbit anti-KMT2D (sc-293217, Santa Cruz), mouse anti-GST (sc-138, Santa Cruz Biotechnology), mouse anti-Flag (F3165, Sigma), rat anti-human SSEA3 DyLight 488 (MC-631, Life Technologies), rabbit anti-Pax6 (AB2237, Millipore), rabbit anti-Ki67 (Abcam, ab15580), goat anti-rabbit IgG (H+L) Alexa Fluor 488 (A11034, Life Technologies), and rat IgG (I4131, Sigma) and rabbit IgG (I5006, Sigma).

For the generation of anti-H3R2me2a antibodies, a peptide encompassing aa 2-9 of histone H3 with an asymmetrically dimethylated arginine (AR(me2)TKQTAR) was coupled to ovalbumin for immunization. Lou/c rats were immunized subcutaneously (s.c.) and intraperitoneally (i.p.) with a mixture of 40 $\mu$ g peptide, 5nmol CpG (TIB Molbiol) and an equal volume of incomplete Freund's adjuvant (Sigma). After 6 weeks, a boost without adjuvant was given i.p. and s.c. 3 days before fusion. Fusion of the myeloma cell line P3X63-Ag8.653 with the immune splenic cells was performed according to the standard procedure described by Koehler and Milstein (Köhler and Milstein, 1975). Hybridoma supernatants were screened in an enzyme-linked immunoassay on biotinylated dimethylated and unmethylated peptides. Supernatants positively tested on dimethylated peptides were further validated by dot plot analysis using H3 peptides (aa 2-9) either unmodified, monomethylated, asymmetrically dimethylated or symmetrically dimethylated at R2. The hybridoma cells of H3R2-reactive supernatants were cloned twice by limiting dilution.

### Plasmids and cloning

The following plasmids were used: pLentiCRISPRv1 (Addgene), pInducer20 (Meerbrey et al., 2011), pGEX-KMT2D PHD<sub>4-6</sub> wild type and mutant (E1516A/E1517A/D1518A/E1544A in PHD<sub>6</sub>) as well as pCMV2-Flag-MLL4 PHD<sub>4-6</sub> C-terminal fusion (Dhar et al., 2012). For design of gRNA (guide RNA), a web-based tool (<http://crispr.mit.edu>) was employed and the following target sites in human *PRMT6* or GFP (as control) were chosen:

gPRMT6.2 (plus strand):	5'-CCGTGCCGCGCTACGCCCCGC-3'
gPRMT6.8 (minus strand):	5'-TTTCTTGGGCTGCGACATCT-3'
gPRMT6.11 (plus strand):	5'-CTCGGACGTTTCGGTCCACG-3'
gPRMT6.12 (plus strand):	5'-CGCACCGATGCCTACCGCCT-3'
gPRMT6.14 (minus strand):	5'-GGTAGGCATCGGTGCGGACG-3'
gPRMT6.15 (plus strand):	5'-GACGGTACTGGACGTGGGCG-3'
Control_gRNA (GFP):	5'-GGAGCGCACCATCTTCTTCA-3'

Pairs of oligo nucleotides for these targeting sites (including the PAM sequence) were annealed and cloned into BsmBI-restricted plentiCRISPRv1 plasmid, which allows bicistronic expression of Cas9 nuclease and gRNA (Shalem et al., 2014).

Human full-length, wild type PRMT6 cDNA with N-terminal 3xFlag-tag (Flag-PRMT6) was amplified by PCR, cloned into the Acc65I and XhoI sites of pENTR4 entry vector and then transferred into pInducer20 via LR recombination (Gateway Cloning System, Invitrogen).

### Production of lentiviral particles and infection of NT2/D1 and U2OS cells

For CRISPR/Cas9-mediated deletion of *PRMT6* in NT2/D1 and U2OS cells and for the overexpression of Flag-PRMT6 (wild type) in NT2/D1 PRMT6 KO cells, HEK293T cells were transfected with the two packaging plasmids pMD2.G and psPAX2 together with the lentiviral expression plasmids encoding either the gRNA/controls and Cas9 (lentiCRISPRv1) or 3xFlag-PRMT6/empty vector (pInducer20). Transfections were performed using X-tremeGENE (Roche). Supernatants containing lentiviral particles were harvested one and two days after transfection and concentrated using PEG. For CRISPR/Cas9 infections, 1.6x 10<sup>5</sup> cells were seeded in a 6-well plate. The next day, cells were infected in the presence of polybrene (8 $\mu$ g/ml) with viruses encoding either the combination of three *PRMT6* gRNAs (gP6\_2, gP6\_11 and gP6\_14 for KO-1; gP6\_8, gP6\_12 and gP6\_15 for KO-2) or the GFP control gRNA (for CT). Cell pools were selected using 1 $\mu$ g/ml puromycin and subjected to serial dilution to generate cell clones. For doxycycline-inducible expression of PRMT6, NT2/D1 KO cells were infected in the presence of polybrene (8 $\mu$ g/ml) with viruses containing either 3xFlag-PRMT6 or the corresponding empty vector. Cell pools

were selected using 800µg/ml G418. To induce PRMT6 expression, cells were treated for 6 days with 1µg/ml doxycycline (D9891, Sigma).

### Synthetic histone peptides, dot blot analysis and peptide pulldown

The following unmodified and modified N-terminal histone H3 and H4 peptides were used:

Name	Length (aa – aa)	C-terminus	Source
H3R2me0	1-8	Cystein	Peptide Specialty Laboratories
H3R2me1	1-8	Cystein	Peptide Specialty Laboratories
H3R2me2a	1-8	Cystein	Peptide Specialty Laboratories
H3R2me2s	1-8	Cystein	Peptide Specialty Laboratories
H3R2me0	1-30	Cystein	Peptide Specialty Laboratories
H3R2me1	1-30	Cystein	Peptide Specialty Laboratories
H3R2me2a	1-30	Cystein	Peptide Specialty Laboratories
H3R17me0	1-24	Biotin/Cystein	Peptide Specialty Laboratories
H3R17me2a	1-24	Biotin/Cystein	Peptide Specialty Laboratories
H3K4me3	1-15	Cystein	Peptide Specialty Laboratories
H3K9me1	1-15	Cystein	Peptide Specialty Laboratories
H3K9me2	1-15	Cystein	Peptide Specialty Laboratories
H3K9me3	1-15	Cystein	Peptide Specialty Laboratories
H3K27me2	1-30	Cystein	Peptide Specialty Laboratories
H4R3me0	1-15	Biotin/Cystein	Peptide Specialty Laboratories
H4R3me2a	1-15	Biotin/Cystein	Peptide Specialty Laboratories
H3R2me2a	1-15	Biotin	Hyllus et al., 2007
H3K4me3	1-15	Biotin	Hyllus et al., 2007
H3R2me2a/K4me3	1-15	Biotin	Hyllus et al., 2007

To monitor the quality and amount of synthesized peptides, 1µg of each was separated by SDS-PAGE and subjected to silver staining as previously described (Chevallet et al., 2006). For dot blot analysis, 1µg of each peptide was spotted onto nitrocellulose membrane, blocked with TBS/0.2% Tween 20/4%BSA for 1 h and stained with rat monoclonal α-H3R2me2a.

For peptide pulldowns, peptides were coupled to SulfoLink resin (Pierce) according to the manufacturer's protocol. Coupled peptides (10µg) were incubated under rotation for 2 h at 4°C with 1µg recombinant GST alone, GST-KMT2D PHD<sub>4-6</sub> (aa 1358-1572) wild type or mutant, which beforehand were expressed in *E. coli* BL21 and purified according to standard procedures. After extensive washes in BC Buffer (20mM HEPES pH 7.9, 150mM NaCl, 0.5% NP40, 20% glycerol, 0.4mM EDTA), bound proteins were analyzed by SDS-PAGE and immunoblotting. Alternatively, peptide pulldowns were performed using HeLa cell extracts overexpressing Flag-MLL4 PHD<sub>4-6</sub> C-terminal fusion protein. Therefore, HeLa cells were transfected using Fugene HD (Promega) according to the manufacturer's protocol. Coupled peptides (10µg) were blocked under rotation with PBS/2% BSA for 30 min and subsequently incubated with 2mg HeLa cell extract under rotation at 4°C for 2 h. After extensive washes in Flag-washing puffer (20mM HEPES pH 7.9, 150mM KCl, 20% glycerol, 0.1% Triton X-100, 0.2mM EDTA), bound proteins were analyzed by SDS-PAGE and immunoblotting.

### Protein isolation and Western Blot

For lysis, cells were resuspended in FT buffer (20mM Tris pH 7.8, 600mM KCl, 20% (v/v) glycerol, 10µg/ml protease inhibitors) and three times frozen and thawed. Cell extracts were subjected to benzonase treatment (0.25U/µl in presence of 7.5mM MgCl<sub>2</sub> for 1 h at 4°C). After centrifugation, cell lysates were analyzed by SDS-PAGE followed by immunoblotting.

### Flow cytometry

For quantification of the cell cycle distribution by flow cytometry, NT2/D1 cells were harvested, washed in ice-cold PBS and fixed in 80% ethanol for 10 min at -20°C. After complete permeabilization, cells were washed again and DNA was stained with 54µM propidium iodide (PI) in the presence of 38mM sodium citrate and 250µg/ml RNase A for 30 min at 37°C. Samples were then analyzed with a Becton Dickinson FACS Calibur. For pluripotency marker

(SSEA3) analysis by flow cytometry, NT2/D1 as well as HeLa cells ( $10^6$  each) were resuspended in PBS/0.5% BSA and stained with DyLight 488-conjugated anti-human SSEA3 at 4°C for 1 h in the dark. After washing (once in PBS, twice in PBS/0.5% BSA) cells were resuspended in PBS and measured with a Becton Dickinson FACS Calibur. Data were analyzed with FlowJo version 7.6.5 (Tree Star) using HeLa cell fluorescence as a negative control.

## Animals

Constitutive *Prmt6*  $-/-$  (KO) mice were provided by the laboratory of Stephane Richards (Neault et al., 2012). For generation of *Prmt6*  $-/-$  (KO),  $+/-$  (HET) and  $+/+$  (WT) embryos of embryonic day 12.5 (E12.5), pregnant female mice (*Prmt6* HET) were sacrificed by cervical dislocation and embryos were decapitated. Embryo heads were fixed for 3 h in 4% PFA at 4°C, then transferred into PBS. For cryoprotection embryo heads were incubated for 2 days in 15% sucrose/PBS followed by incubation for 2 days in 30% sucrose/PBS before freezing on dry ice and storage at  $-80^{\circ}\text{C}$ . For immunofluorescence (IF) staining, embryo heads were cut into 20  $\mu\text{m}$ -thick coronal sections using Leica microtome CM3050S. Sections were postfixed (10 min in 4% PFA), washed twice for 5 min each in 50mM glycine and in PBS before incubating for 60 min in blocking solution (2% BSA, 3% goat serum, 0.5% NP40 in PBS). Incubation with primary antibodies (anti-Pax6 1:200 and anti-Ki67 1:50) was performed overnight at 4°C in blocking solution without goat serum. Subsequently, sections were washed 3x with PBS, blocked for 30 min in blocking solution and then secondary antibodies were supplied for 2 h. Finally, the sections were counter-stained with 5  $\mu\text{g}/\text{ml}$  Propidium-Iodid (Sigma P4170) for 15 min, washed 3x with PBS and embedded in DABCO medium and stored at 4°C. Fluorescence images were acquired using confocal Leica TCS SP5 II microscope (20x Leica objective) and the software Leica LAS AF as well as Fiji. Neural progenitor cell numbers (Pax6- or Ki67-positive cells) were quantified from a standardized area (125 x 125  $\mu\text{m}$  at 50-fold magnification) of 5-6 embryos of each condition. The VZ layer width (Pax6-positive) as well as the VZ/SVZ layer width (Ki67-positive) was measured at three positions of four independent pictures of each embryo (5-6 embryos per condition) and the mean layer width was calculated.

## RNA isolation and reverse transcription quantitative PCR (RT-qPCR)

Total RNA was isolated using RNA-Mini-Kit (SeqLab, Göttingen, Germany). For cDNA synthesis 0.5-1  $\mu\text{g}$  of total RNA was used as template for random hexamer oligonucleotides and M-MLV reverse transcriptase (Thermo Scientific) according to the manufacturer's instruction. cDNA was subjected to PCR amplification using different primers (listed below) and Absolute qPCR SYBR Green Mix (Thermo Scientific).

Forward (fwd) and reverse (rev) primers used for RT-qPCR of indicated gene transcripts:

Name	Sequence (5'-3')
hARID1A RT fwd	CCAACAAAGGAGCCACCA
hARID1A RT rev	TTGCCCATCTGATCCATTG
hCNOT1 RT fwd	TGCAGCAGTATGATCTTCACCT
hCNOT1 RT rev	CATCCACCAGCAGGATTTTT
hCRABP1 RT fwd	TCAACTTCAAGGTCGGAGAAG
hCRABP1 RT rev	TCATTCTCCCAAGTGGCTAAA
hID1 RT fwd	CCAGAACCGCAAGGTGAG
hID1 RT rev	GGTCCCTGATGTAGTCGATGA
hLARS RT fwd	TGACAAATTTTCAGCAGATGGA
hLARS RT rev	GGCATCTTCTACAGTGTACCA
hMITF RT fwd	CAAAAGTCAACCGCTGAAGA
hMITF RT rev	AGGAGCTTATCGGAGGCTTG
hNANOG RT fwd	TCCAGCAGATGCAAGAATC
hNANOG RT rev	TTGCTATTCTTCGGCCAGTT
hOCT4 RT fwd	TGAAGAACAAGTGCCAAATAGC
hOCT4 RT rev	GCGGCTATACAAAGTGGACAA
hPSMF1 RT fwd	GTTACTTCGGCTTGGGTGTC
hPSMF1 RT rev	CATACAGGTCTTTATTGTTGTTCCA
hRP11-834C11.4 RT fwd	GGAAATCTAGATGAGCCTGTCC
hRP11-834C11.4 RT rev	CTGCTCACCAAGGTCTGGA
hST3GAL2 RT fwd	GTCTGGACCCGAGAGAACAT
hST3GAL2 RT rev	TGGTGTGTGTGACTTGAAGT
hUBC RT fwd	CACTTGGTCCTGCGCTTGA



hUBC RT rev	CAATTGGGAATGCAACAACCTTTAT
hVTCN1 RT fwd	GCAGATCCTCTTCTGGAGCAT
hVTCN1 RT rev	CCAGCTGAGGCGACAGTAGT

For RNA sequencing (RNA-seq), total RNA was isolated from three biological replicates using RNA-Mini-Kit. RNA quality was assessed using the Experion RNA StdSens Analysis Kit (BioRad). RNA-seq libraries were prepared from total RNA using the TruSeq Stranded mRNA LT kit (Illumina) according to the manufacturer's instructions. Quality of sequencing libraries was controlled on a Bioanalyzer 2100 using the Agilent High Sensitivity DNA Kit (Agilent). Pooled sequencing libraries were quantified with digital PCR (QuantStudio 3D, Thermo Fisher) and sequenced on the HiSeq 1500 platform (Illumina) in Rapid-Run mode with 50 base single reads.

### Chromatin immunoprecipitation and quantitative PCR (ChIP-qPCR) and ChIP-seq

For immunoprecipitation of histone marks, cells were crosslinked for 10 min with 1% formaldehyde at room temperature. For immunoprecipitation of KMT2A and KMT2D, disuccinimidyl glutarate (DSG) was added at a final concentration of 2mM to the cells and incubated 45 min at room temperature. After 2 washings in PBS, cells were crosslinked with formaldehyde as described above. The reaction was stopped by addition of glycine at a final concentration of 0.125M for 5 min. For KMT2D ChIP, cells were lysed in Lysis buffer B (10mM HEPES/KOH pH6.5, 10mM EDTA, 0.5mM EGTA, 0.25% Triton X 100) for 10 min on ice, centrifuged and resuspended in Lysis buffer C (10mM HEPES/KOH pH6.5, 10mM EDTA, 0.5mM EGTA, 200mM NaCl). After a 20 min incubation on ice and centrifugation, Lysis buffer D (50mM Tris/HCl pH 8.5, 10mM EDTA, 1% SDS, protease inhibitors) was added to the cells and incubated for 20 min on ice. Nucleic lysates were sonified using the Bioruptor (Diagenode) for 2 times 7 min (30 sec ON, 30 sec OFF; HIGH amplitude). After centrifugation, 100µg chromatin was subjected to the OneDay ChIP Kit (Diagenode) according to the manufacturer's instructions. For the other factors and for histone modifications, cell lysis was performed in Lysis buffer I (5mM PIPES pH 8, 85mM KCl, 0.5% NP-40, protease inhibitors) for 10 min on ice. After centrifugation, cell pellets were resuspended in Lysis buffer II (10mM Tris/HCl pH 7.5, 150mM NaCl, 1% NP-40, 1% sodium deoxycholate, 0.4% SDS, 1mM EDTA, protease inhibitors) and incubated on ice for 20 min. Chromatin was fragmented at 4°C by sonification using a Branson Sonifier W-250-D (80x 1 sec, 3 sec pause, 15% amplitude). Subsequently, 100µg chromatin were precleared with blocked Protein A or Protein G Sepharose (1mg/ml BSA and 400µg/ml salmon sperm DNA in Lysis buffer II) for 2 h at 4°C. For immunoprecipitations except H3R2me2a, 4µg of antibodies were added to the precleared chromatin and incubated overnight at 4°C. To immobilize immunoprecipitates, 60µl of Protein A Sepharose were added for 2 h at 4°C and subjected to successive washing steps. For anti-H3R2me2a immunoprecipitations, 1-2ml hybridoma supernatant was incubated with blocked Protein G beads for 2 h at 4°C. After washes in Lysis buffer II, antibodies-precoupled beads were added to 100µg of precleared chromatin and incubated overnight at 4°C. The next day, immobilized immunoprecipitates were washed twice with washing buffer I (20mM Tris/HCl pH 8.1, 150mM NaCl, 2mM EDTA, 0.1%SDS, 1%Triton X-100), washing buffer II (20mM Tris/HCl pH 8.1, 500mM NaCl, 2mM EDTA, 0.1% SDS, 1% Triton X-100), washing buffer III (10mM Tris/HCl pH 8.1, 250mM LiCl, 1mM EDTA, 0.1% sodium deoxycholate, 1% NP-40) and TE buffer. Chromatin was eluted twice with 250µl 0.1M NaHCO<sub>3</sub> and 1% SDS for 15 min at RT. Crosslinking was reversed by incubation with 1µl of 10mg/ml Proteinase K and RNase A for 3 h at 55°C followed by overnight at 65°C. DNA was purified *via* QIAquick columns (QIAGEN) and either processed for ChIP-seq or analyzed by ChIP-qPCR using different primers (listed below) and Absolute qPCR SYBR Green Mix (Thermo Scientific). For ChIP-seq, libraries were prepared according to the manufacturer's protocol (Diagenode, MicroPlex Library Preparation Kit).

Forward (fwd) and reverse (rev) primers used for ChIP-qPCR of indicated genomic loci, either amplifying the specific PRMT6 binding site (=spec) or a corresponding control region (=ctr):

Name	Sequence (5'-3')
ARID1A ChIP spec fwd	GTGAGGGAGAGCTAGCGAGA
ARID1A ChIP spec rev	GCGCAGATTGGAGAACTAGG
ATG4C ChIP spec fwd	TTGGGTTGGCTCTATCTTGG
ATG4C ChIP spec rev	TCCTCTCGAGCACTTGGACT
ATG4C ChIP CT fwd	GGCAAAACCCCATCTCTACA
ATG4C ChIP CT rev	TTGATCTCCCAGGCTCAAGT
C12orf57 ChIP spec fwd	TTTTGGTGGTCTTGATGCAG
C12orf57 ChIP spec rev	GTTCAGCGGAGGTAAATGGA

CLEC16A ChIP spec fwd	TAGTCCGTTTCGCGGAGTC
CLEC16A ChIP spec rev	CAGCCCAGCACTGACATTC
CNOT1 ChIP spec fwd	AAGCAAGCCAGGTTGTGACT
CNOT1 ChIP spec rev	GTGACTACAACCCCCAGCAT
CNOT1 ChIP ctr fwd	CCAGGCAATGACCAATTCTT
CNOT1 ChIP ctr rev	AATCAGTGCCCTTTTGATGG
CRABP1 ChIP spec fwd	TTGATCGGGAGAGAGAATGG
CRABP1 ChIP spec rev	CTGCAGGAGCCAGAGACAA
CRABP1 ChIP K4me1spec fwd	AGCAGCGACCAGACCAAG
CRABP1 ChIP K4me1spec rev	TTCACCCCACCTCACTTAG
FASTKD1 ChIP spec fwd	GAGACATGACCTTTCCCATGA
FASTKD1 ChIP spec rev	ACGTCCATTTCACCCACCT
FASTKD1 ChIP CT fwd	TTCCTGTCTGGTTTCCATTG
FASTKD1 ChIP CT rev	AAGGCAAATGTTAGGGAGGAA
ID1 ChIP spec fwd	CGCACTCTCATTCCACGTT
ID1 ChIP spec rev	TTCATGATTCTTGGCGACTG
KDM5A ChIP spec fwd	TCTTGCAAGGCTTTTCCACT
KDM5A ChIP spec rev	GAAGGAAAGGCCAGACACAC
KDM5A ChIP CT fwd	TTTTCGGTTTCCTGGTACATAAA
KDM5A ChIP CT rev	CAGAGCAAGACTCTGTCTCAAAAA
LARS ChIP spec fwd	GTCTACCCGATAGGCCCACT
LARS ChIP spec rev	GCACTGCATCATGGACTTTG
LARS ChIP ctr fwd	CAAGCCAATGTTCTGCTTCA
LARS ChIP ctr rev	CCAGTGGGGCATTATGAAAT
MITF ChIP spec fwd	AGCAAGTGGGGAGAGAGGA
MITF ChIP spec rev	GCTCCCACGAAAACCTACAGC
NUDCD1 ChIP spec fwd	TCGCACAGAGACTGGGAAG
NUDCD1 ChIP spec rev	CTACATAGCCCAGCATGCAA
NUDCD1 ChIP CT fwd	TTTGCAGAGTTCTCCCAAAAA
NUDCD1 ChIP CT rev	TCTTCTTCTCAACCCTTACAAAGA
OCT4 ChIP spec fwd	AAGAAGCCTGGGAGGGACT
OCT4 ChIP spec rev	GTTAGAGCTGCCCCCTCTG
PHF12 ChIP spec fwd	CAACGCCAAAGGGTCTAAAG
PHF12 ChIP spec rev	GACTCTTCCCCGGGTCTATC
PHF12 ChIP CT fwd	CCCAACAAAATCAAGAGAGCA
PHF12 ChIP CT rev	CTGAGGCAGGAGAATCAGTTG
PSMF1 ChIP spec fwd	ATGTGGACGGTAGCAAGCA
PSMF1 ChIP spec rev	CACCTTGCTGAGAGGCAGA
RP11-834C11.4 ChIP spec fwd	GGCCAGGATTAACCACAGAA
RP11-834C11.4 ChIP spec rev	ACACTGTCCAGAGCCCAGAC
RP11-834C11.4 ChIP K4me1spec fwd	GCAGAGGGATTGCTCAACAT
RP11-834C11.4 ChIP K4me1spec rev	TGGACTGTGAGGGACACAAA
SNX12 ChIP spec fwd	TCATAGGTGGTGAAGCGCG
SNX12 ChIP spec rev	CCGCCAAGTAACTTCCTGGA
ST3GAL2 ChIP spec fwd	GCATGCTGGGATATGGAGTC
ST3GAL2 ChIP spec rev	CGCTGTCTTCTGGGAGATGT
ST3GAL2 ChIP CT fwd	GAGTGCAGTGGTGCGATCT
ST3GAL2 ChIP CT rev	AAAATTAGCCAGGCATGGTG
VTCN1 ChIP spec fwd	GGAAGTAGGCCCCAAAAGAG
VTCN1 ChIP spec rev	CTGTCAGGCCATCCATCTG
VTCN1 ChIP K4me1spec fwd	TCCAGGGCACCAGTCTTAGT
VTCN1 ChIP K4me1spec rev	CCATCTCCAGGTCAGTGTCA

## Bioinformatic analysis

### ChIP-seq

Replicate samples were sequenced as single-end reads using an Illumina HiSeq 1500. Reads were de-multiplexed using Illumina bcl2fastq and aligned with Bowtie2 (Langmead and Salzberg, 2012) against *Homo sapiens*, release 74, Ensembl genome. After alignment de-duplication was performed to remove PCR duplicates. For visualization, de-duplicated BAM files were converted to TDF with parameter (window\_size = 10) using IGV tools and visualized using IGV 2.3.82 (Robinson et al., 2011) with option import as normalized tracks for some profiles mentioned in the corresponding legends. Peak calling was performed using MACS (Zhang et al., 2008). All peaks were called accounting the background with corresponding IgG control ChIP-seq data. Peaks were further filtered with criteria  $\geq 35$  tag counts and  $\geq 2$ -fold enrichment above IgG and density-based criteria (peak length/tag count  $\leq 15$ ). Heatmaps were created with custom script where read density data were extracted in 60 bins 100bp/bin from -3kb to +3kb by keeping the corresponding peak summit as centre. To further investigate the structure in data, k-means clustering (algorithm=auto, distance metric=euclidean, number of cluster=10, iterations=1000) in scikit-learn was employed. The read coverage was normalized by dividing with total read count, multiplying by one million and then plotted with R, heatmap3 package. In Fig. 3A and Fig. S5C normalization constant between CT and KO ChIP-seq was calculated by resampling all H3K4me3 peaks (assuming that the majority of H3K4me3 was not affected by PRMT6 loss) in a subset with replacement and this process was repeated for 10000 iteration. Normalization constant was calculated as the mean difference between CT and KO for 10000 iterations. In the boxplot analysis (Fig. 4B, Fig. S6F) tag densities for the H3K4me3, H3K4me1, H3K27ac and KMT2D samples were retrieved  $\pm 2$ Kb from the summit of H3R2me2a peaks and normalized. In Figure S6 (A, B, G and H), normalized tag densities for H3R2me2a, H3K4me1, H3K27ac and KMT2D in + ATRA and - ATRA conditions were divided to obtain the fold change of enrichment. These fold changes were used in calculating the Spearman correlation coefficient between two histone modifications.

### RNA-seq

Samples were prepared as biological triplicates and sequenced as single-end reads using an Illumina HiSeq 1500. Reads were aligned with Tophat2 (Kim et al., 2013) against *Homo sapiens*, release 74, Ensembl genome. Read coverage (number of overlapping reads per base pair) was calculated over non-overlapping exons. The exon counts were aggregated for each gene to build a read count table using SubRead function featureCount (Liao et al., 2013). Differentially regulated genes were calculated using DESeq2 (Love et al., 2014). For differentially regulated genes a threshold ( $FC \geq 2$  or  $FC \leq -2$ , adj-pval  $\leq 0.01$ ) was followed. To analyze the biological significance of genes, Metascape (<http://metascape.org>) (Tripathi et al., 2015) was used for gene ontology analysis. We normalized expression data with transcript per million (TPM) (Wagner et al., 2012) for quantile based binning of genes expression. For significance testing of differences between two sample distributions Welch's t-test was employed.

### External Datasets

SRR1204514: H3K4me3 U2OS

SRR2558762: H3K4me1 U2OS

SRR1204515: H3K27ac U2OS

## Supplemental References

Chevallet, M., Luche, S., and Rabilloud, T. (2006). Silver staining of proteins in polyacrylamide gels. *Nat. Protoc.* *1*, 1852–1858.

Dhar, S.S., Lee, S.H., Kan, P.Y., Voigt, P., Ma, L., Shi, X., Reinberg, D., and Lee, M.G. (2012). Trans-tail regulation of MLL4-catalyzed H3K4 methylation by H4R3 symmetric dimethylation is mediated by a tandem PHD of MLL4. *Genes Dev.* *26*, 2749–2762.

Hyllus, D., Stein, C., Schnabel, K., Schiltz, E., Imhof, A., Dou, Y., Hsieh, J., and Bauer, U.-M. (2007). PRMT6-mediated methylation of R2 in histone H3 antagonizes H3 K4 trimethylation. *Genes Dev.* *21*, 3369–3380.

Kim, D., Pertea, G., Trapnell, C., Pimentel, H., Kelley, R., and Salzberg, S.L. (2013). TopHat2: accurate alignment of transcriptomes in the presence of insertions, deletions and gene fusions. *Genome Biol.* *14*, R36.

Köhler, G., and Milstein, C. (1975). Continuous cultures of fused cells secreting antibody of predefined specificity. *Nature* *256*, 495–497.

Langmead, B., and Salzberg, S.L. (2012). Fast gapped-read alignment with Bowtie 2. *Nat. Methods* *9*, 357–359.

Liao, Y., Smyth, G.K., and Shi, W. (2013). The Subread aligner: Fast, accurate and scalable read mapping by seed-and-vote. *Nucleic Acids Res.* *41*.

Love, M.I., Huber, W., and Anders, S. (2014). Moderated estimation of fold change and dispersion for RNA-seq data with DESeq2. *Genome Biol.* *15*, 550.

Meerbrey, K.L., Hu, G., Kessler, J.D., Roarty, K., Li, M.Z., Fang, J.E., Herschkowitz, J.I., Burrows, A.E., Ciccio, A., Sun, T., et al. (2011). The pINDUCER lentiviral toolkit for inducible RNA interference in vitro and in vivo. *Proc. Natl. Acad. Sci.* *108*, 3665–3670.

Robinson, J.T., Thorvaldsdóttir, H., Winckler, W., Guttman, M., Lander, E.S., Getz, G., and Mesirov, J.P. (2011). Integrative Genome Viewer. *Nat. Biotechnol.* *29*, 24–26.

Shalem, O., Sanjana, N.E., Hartenian, E., Shi, X., Scott, D.A., Mikkelsen, T.S., Heckl, D., Ebert, B.L., Root, D.E., Doench, J.G., et al. (2014). Genome-Scale CRISPR-Cas9 Knockout Screening in Human Cells. *Science* (80- ). *343*, 84–87.

Tripathi, S., Pohl, M.O., Zhou, Y., Rodriguez-Frandsen, A., Wang, G., Stein, D.A., Moulton, H.M., Dejesus, P., Che, J., Mulder, L.C.F., et al. (2015). Meta- and Orthogonal Integration of Influenza “oMICs” Data Defines a Role for UBR4 in Virus Budding. *Cell Host Microbe* *18*, 723–735.

Umlauf, D., Goto, Y., Delaval, K., Wagschal, A., Arnaud, P., and Feil, R. Chromatin immunoprecipitation on native chromatin from cells and tissues (PROT22). 2005. Epigenome Network of Excellence. [www.epigenome-noe.net](http://www.epigenome-noe.net)

Wagner, G.P., Kin, K., and Lynch, V.J. (2012). Measurement of mRNA abundance using RNA-seq data: RPKM measure is inconsistent among samples. *Theory Biosci.* *131*, 281–285.

Zhang, Y., Liu, T., Meyer, C.A., Eeckhoutte, J., Johnson, D.S., Bernstein, B.E., Nussbaum, C., Myers, R.M., Brown, M., Li, W., et al. (2008). Model-based Analysis of ChIP-Seq (MACS). *Genome Biol.* *9*, R137.